Formation and Structure of Porous Gel Networks from $Si(OMe)_4$ in the Presence of $A(CH_2)_nSi(OR)_3$ (A = Functional Group)

Nicola Hüsing and Ulrich Schubert*

Institut für Anorganische Chemie, Technische Universität Wien, Getreidemarkt 9, A-1060 Wien, Austria

Klaus Misof and Peter Fratzl†

Institut für Materialphysik, Universität Wien, Boltzmanngasse 5, A-1090 Wien, Austria

Received March 16, 1998. Revised Manuscript Received March 27, 1998

Monolithic silica aerogels modified by functional organic groups were prepared by sol−gel processing of $Si(OMe)_4/A(CH_2)_nSi(OR)_3$ mixtures under identical experimental conditions, followed by drying of the wet gels with supercritical CO_2. The employed functional groups A were SH ($n = 3$), $OCH_2\overline{CHCH_2O}$ ($n = 3$), $OC(O)C(Me)=CH_2$ ($n = 3$), NCO ($n = 3$), Cl ($n = 3$), NHC(O)OMe ($n = 3$), and PPh_2 ($n = 2$). These groups were retained in the aerogels except the isocyanate groups, which reacted with methanol to the corresponding carbamate. The properties of the obtained aerogels are rather independent of the kind of functional group, but strongly depend on the $Si(OMe)_4/A(CH_2)_nSi(OR)_3$ ratio, which was varied between 9:1 and 6:4. The density of the aerogels was 0.2−0.3 g cm^{-3}; some aerogels with lower densities were also prepared for comparison. Gelling of the precursor mixtures is drastically slowed with an increasing portion of $A(CH_2)_nSi(OR)_3$, and the water consumption is retarded. During supercritical drying, shrinkage of ∼10% was observed for the aerogels prepared from the 9:1 precursor mixtures. Increasing the portion of $A(CH_2)_nSi(OR)_3$ or decreasing the aerogel density lead to a larger shrinkage and an incomplete incorporation of the functional organic groups. The chemical composition of the resulting aerogels was investigated by infrared (IR) and Raman spectroscopy, elemental analysis, and titration of the functional groups, and their structure by nitrogen sorption and small-angle X-ray scattering (SAXS). The Brunauer−Emmett−Teller (BET) surface areas generally decreased with an increasing portion of $A(CH_2)_nSi(OR)_3$, whereas the *C* parameter showed a saturation behavior. An analysis of the pore volumes indicated that with an increasing portion of $A(CH_2)_nSi(OR)_3$ or a decreasing bulk density, the gel skeleton is increasingly compressed during the N_2 sorption experiments. SAXS measurements showed larger particles upon increasing the $A(CH_2)_n$-$Si(OR)_3/Si(OMe)_4$ ratio, which correlates with the observed decrease of the specific surface areas. The results were interpreted that an increasing portion of $A(CH_2)_nSi(OR)_3$ has the same kinetic effects on the hydrolysis and condensation reactions and the same structural consequences for the network formation as decreasing the bulk density of an aerogel obtained from the one-component $Si(OMe)_4$ system. The fractal dimension increased with an increasing portion of $A(CH_2)_nSi(OR)_3$; it was significantly larger for A = NCO and NHC(O)OMe than for A = SH or $OC(O)C(Me)=CH_2$.

Introduction

Porous inorganic materials have found widespread attention for a variety of applications such as catalysts, separation media, membranes or sensors.[1] Much work has already been accomplished in the controlled chemical synthesis and design of structures and porosity in materials from the micro- to the macroporous range, such as the development of the new mesoporous solids.[2]

For several potential technical applications, such as chromatography, sensors, or immobilization of enzymes or metal complexes, solids with reactive sites at their inner surface, not just porous inorganic materials, are required. As a consequence, a controlled processing of inorganic precursors in the presence of functionalizing agents is necessary to achieve both a tailored microstructure and porosity and a deliberate positioning of the reactive sites.

The sol−gel process is a very powerful approach to the preparation of organically modified inorganic ma-

† New address: Erich Schmid Institut der Österreichischen Akademie der Wissenschaften & Montanuniversität Leoben, Jahnstr. 12, A-8700 Leoben, Austria.

(1) Schaefer, D. W. *MRS Bull.* **1994**, *24(4)*, 14.

(2) Kresge, C. T.; Leonowicz, M. E.; Roth, W. J.; Vartuli, J. C.; Beck, J. S. *Nature* **1992**, *359*, 710. Behrens, P.; Stucky, G. D. *Compr. Supramol. Chem.* **1996**, *7*, 721.

10.1021/cm980706g CCC: $15.00
Published on Web 08/13/1998

terials with a tailored microstructure. Especially for silica systems, the synthesis of inorganic−organic hybrid materials was very well investigated. However, surprisingly little attention has been paid to an understanding of the processing−structure relationships in these systems that is necessary for a rational design.

Aerogels are materials in which the structure of the wet gel can be largely preserved if supercritical drying is performed with liquid carbon dioxide as a fluid. Obviously, this material represents an excellent example to correlate the chemistry during sol−gel processing with the structural characteristic of the gel network.[3] Sol−gel derived and supercritically dried inorganic−organic hybrid silica aerogels modified with alkyl and aryl groups were previously prepared by us starting from $R'Si(OR)_3/Si(OR)_4$ mixtures (R′ = alkyl, aryl).[4] The filigrane network and the extreme porosity typical for aerogels require a very careful control of the sol−gel chemistry. We showed in the previous studies that the modification with simple alkyl or aryl groups lead to an improvement of the hydrophobicity and the compliance of the aerogel. Additionally, the organic groups were used to create nanometer-sized carbonaceous structures by pyrolysis to improve the heat insulation properties of the aerogels.[5]

Raman spectroscopy allowed a first insight into the sol−gel reactions of such two-component systems. It was clearly demonstrated that in base-catalyzed reactions, the tetraalkoxysilane reacts first, building up the backbone of the silica gel while the organically modified precursor is acting basically as a cosolvent. The trialkoxysilane is hydrolyzed in a later stage of the reaction and condensed to the surface of the then existing silica structures.[6]

In an extension of this previous work, we have now incorporated functional organic groups into the aerogels by the same approach using organofunctional alkoxysilanes of the type $A(CH_2)_nSi(OR)_3$ (A = functional organic group).[7] Such aerogels are very promising materials for new types of sensors, catalysts, adsorbents, etc. In this paper, we mainly address the question whether and how the silicon-bonded organic groups influence the build-up and structure of the gel network. We restrict ourselves to alkoxysilanes without amino substituents. Owing to the higher basicity of the amino groups, alkoxysilane mixtures containing aminoalkyl(trialkoxy)silanes show a different behavior that will be treated elsewhere.[8]

Scheme 1. Trialkoxysilanes of the Type $A(CH_2)NSi(OR)_3$ Used in This Work and Their Acronyms

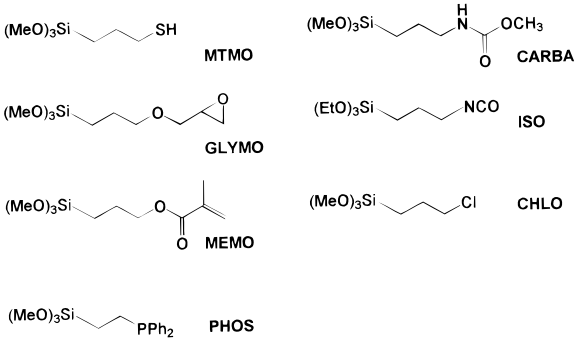

Table 1. Preparation of the Wet Gels

sample	$Si(OMe)_4$ [g (mmol)]	$R'Si(OR)_3$ [g (mmol)]	MeOH [g (mmol)]	0.01 N NH_4OH [g (mmol)]	gel time (t_g) [min]
MTMO 10	20.55 (135)	2.95 (15)	13.22 (413)	10.53 (585)	25
MTMO 20	16.59 (109)	5.30 (27)	15.41 (481)	9.32 (518)	65
MTMO 40	10.50 (69)	9.03 (46)	18.72 (584)	7.46 (414)	180
GLYMO 10	19.33 (127)	3.31 (14)	14.44 (451)	9.90 (550)	50
GLYMO 20	14.92 (98)	5.91 (25)	17.08 (533)	8.41 (467)	65
GLYMO 40	8.83 (58)	9.22 (39)	20.98 (655)	6.28 (349)	410
MEMO 10	19.03 (125)	3.48 (14)	14.60 (456)	9.76 (542)	40
MEMO 20	14.46 (95)	5.96 (24)	17.50 (546)	8.14 (452)	80
MEMO 40	8.52 (56)	9.19 (37)	21.26 (664)	6.03 (335)	250
CHLO 10	20.48 (135)	2.96 (15)	13.34 (416)	10.53 (585)	30
CHLO 20	16.44 (108)	5.35 (27)	15.69 (490)	9.24 (513)	150
CHLO 40	10.41 (68)	9.04 (46)	19.07 (595)	7.38 (410)	205
CARBA 10	19.32 (127)	3.36 (14)	14.24 (444)	9.90 (550)	
CARBA 20	14.89 (98)	5.82 (25)	16.87 (526)	8.41 (467)	
ISO 10	20.26 (133)	3.66 (15)	12.86 (401)	10.39 (577)	210
ISO 20	16.19 (106)	6.58 (27)	14.67 (458)	9.09 (505)	720
ISO 40	10.05 (66)	10.39 (44)	17.46 (545)	7.13 (396)	
PHOS 10	16.93 (111)	4.18 (12)	16.41 (512)	8.64 (480)	45
PHOS 20	11.96 (79)	6.64 (20)	19.75 (616)	6.77 (376)	90

Experimental Section

Sol−Gel Processing of $R'Si(OR)_3/Si(OR)_4$ Mixtures. The aerogels were prepared as previously described.[4] The trialkoxysilanes of the type $A(CH_2)_nSi(OR)_3$ employed in the present work are shown in Scheme 1. 2-Phosphinoethyl(trimethoxy)silane and 3-carbamatopropyl(trimethoxy)silane were prepared according to the methods described by Niebergall and Berger.[9] Tetramethoxysilane (TMOS), the silane $A(CH_2)_nSi(OR)_3$ ($R'Si(OR)_3$), and methanol were mixed in a flask. An amount of methanol was added corresponding to a theoretical density of the final aerogel of 0.200 g cm^{-3} ($d_{theor} = [(1 - x)\, m_{SiO_2} + x m_{R'SiO_{3/2}}]/(V_{Si(OMe)_4} + V_{R'Si(OMe)_3} + V_{H_2O} + V_{ROH}$). To start the sol−gel reactions, an aqueous 0.01 N NH_4OH solution was added, corresponding to the amount of water that is necessary for a complete hydrolysis of the alkoxy groups. The experimental conditions are specified in Table 1. The sol was stirred for 5 min and then transferred to cylindrical polyethylene vessels that were 1.5 cm in diameter and 4.5 cm in height.

Supercritical Drying of the Wet Gels. The resulting gels were aged without solvent exchange at 30 °C before supercritical drying. After a constant aging period of 7 days (starting from the time of adding water), supercritical drying was performed with a Polaron 3100 critical point dryer. The alcohol was first replaced by carbon dioxide, then the temperature and pressure were raised above the critical point of carbon dioxide (T_c = 31 °C, P_c = 7.29 MPa). The resulting aerogels were monolithic cylinders and had the typical aerogel properties with low densities and high porosities.

(3) Hüsing, N.; Schubert, U. *Angew. Chem.* **1998**, *110*, 22; *Angew. Chem., Int. Ed. Engl.* **1998**, *37*, 22.

(4) Schwertfeger, F.; Glaubitt, W.; Schubert, U. *J. Non-Cryst. Solids* **1992**, *145*, 85. Schubert, U.; Schwertfeger, F.; Hüsing, N.; Seyfried, E. *Mater. Res. Soc. Symp. Proc.* **1994**, *346*, 151. Schwertfeger, F.; Hüsing, N.; Schubert, U. *J. Sol-Gel Sci. Technol.* **1994**, *2*, 103. Hüsing, N.; Schwertfeger, F.; Schubert, U.; Tappert, W. *J. Non-Cryst. Solids* **1995**, *186*, 37.

(5) Schwertfeger, F.; Kuhn, J.; Bock, V.; Arduini-Schuster, M. C.; Seyfried, E.; Schubert, U.; Fricke, J. *Thermal Cond.* **1994**, *22*, 589. Schwertfeger, F.; Schubert, U. *Chem. Mater.* **1995**, *7*, 1909.

(6) Hüsing, N.; Schubert, U.; Riegel, B.; Kiefer, W. *Mater. Res. Soc. Symp. Proc.* **1996**, *435*, 339. Riegel, B.; Plitterdorf, S.; Kiefer, W.; Hüsing, N.; Schubert, U. *J. Mol. Struct.* **1997**, *410 & 411*, 157.

(7) Preliminary report: Hüsing, N.; Schubert, U. *J. Sol-Gel. Sci. Technol.* **1997**, *8*, 807.

(8) Hüsing, N. Ph.D. Thesis, University of Würzburg, **1997**. Hüsing, N.; Schubert, U.; Mezei, R.; Fratzl, P.; Riegel, B.; Kiefer, W.; Mader, W. *Chem. Mater.*, submitted.

(9) Niebergall, H. *Makromol. Chem.* **1962**, *52*, 218. Berger, A. U.S. Patent 3,821,218, 1974.

Table 2. Structural Characteristics of the Organofunctional Aerogels

		nitrogen sorption		small-angle X-ray scattering		
sample	optical appearance	BET surface area, [m^2 g^{-1}]	*C* parameter	particle radius, *R* [nm]	fractal dimension, *D*	$3/(R\sigma)$ [g cm^{-3}]
MTMO 10	transparent	638	60	3.44	1.64	1.37
MTMO 20	translucent	550	46	4.15	1.46	1.32
MTMO 40	turbid	321	36	8.02	0.69	1.17
GLYMO 10	translucent	576	52			
GLYMO 20	turbid, translucent	478	43			
GLYMO 40	milky, translucent	427	40			
MEMO 10	translucent	582	52	3.81	1.45	1.35
MEMO 20	turbid, translucent	473	40			
MEMO 40	milky, translucent	414	36			
CHLO 10	yellowish, transparent	310	35			
CHLO 20	yellowish, translucent	583	45			
CHLO 40	yellowish, translucent	502				
CARBA 10	opaque	531	67	3.18	2.45	1.78
CARBA 20	opaque	445	52	5.38	2.36	1.25
ISO 10	opaque	411	69	4.35	2.25	1.68
ISO 20	opaque	346	56	4.79	2.02	1.81
ISO 40	opaque	175	49	11.02	1.39	1.56
PHOS 10	opaque	340	34	8.47	1.81	1.04
PHOS 20	opaque	151	17	8.75	1.84	2.27

The samples are labeled as follows: The letters identify the kind of functional unit incorporated into the silica matrix by using the acronym of the parent silane (Scheme 1). The following number represents the portion of $R'Si(OR)_3$ (in mol %) in the starting mixture of the alkoxysilanes. In a few cases, the theoretical density of the aerogels was varied. The theoretical density (in $10^3 \times$ g cm^{-3}) is indicated by a second number separated by "/". For example, ISO 20/100 is an aerogel prepared from a mixture of 80 mol % $Si(OMe)_4$ and 20 mol % $(EtO)_3Si(CH_2)_3NCO$, with a theoretical density of 0.100 g cm^{-3}. If no density is specified in the label, the theoretical density was 0.200 g cm^{-3}.

Characterization. The physical data for the aerogels are given in Table 2.

The shrinkage during aging and drying was determined by measuring the dimensions of the cylindrical gel body before and after drying. The bulk density was calculated from the mass and the volume of the monolithic samples. The composition of the aerogels was determined by elemental analysis of C, S, P, N, Si, and H. Additionally, the double bonds of MEMO and the mercapto units of MTMO were titrated in a manner analogous to methods described in the literature.[10] Karl Fischer titrations were performed with a Mettler DL18 Karl Fischer Titrator. Thermal measurements were carried out with a Shimadzu DSC-50 and TGA-50 analyzer in an oxygen-containing atmosphere.

A Micromeritics Sorptomat ASAP 2400 was used for the nitrogen sorption studies. The samples were preheated overnight at 110 °C before each measurement. The specific surface area was determined by the Brunauer−Emmett−Teller (BET) method at 77.4 K in the partial pressure range of $0.01 < P/P_0 < 0.25$ (five-point BET). The total pore volume was obtained from the N_2 desorption isotherm. For the calculation of the *C* parameter, only the pressure range of $0.05 < P/P_0 < 0.25$ was used.

Small angle scattering (SAXS) measurement were performed using a pinhole camera with a rotating anode generator and an area detector (Fa. AXS, Karlsruhe). All SAXS patterns were first corrected for background scattering from the experimental setup and then radially averaged to obtain the function $I(q)$, where $q = 4\pi/\lambda$) sin is the scattering vector, 2θ being the angle between the incident and the diffracted beam and $\lambda = 0.154$ nm being the X-ray wavelength. Spectra were obtained in the *q*-range from 0.15 to 9 nm^{-1} by combining data measured for two different sample−detector distances. The setup and its use for the investigation of porous materials are described in refs 11 and 12.

Following Emmerling et al.,[13] the SAXS data were fitted using the following expression:

$$I(q) = I_0[B + V_0 S(q) P(q)]$$

where I_0 is a normalization constant depending on the setup, B is a constant background from the sample, V_0 is the mean volume of the primary particles, $P(q)$ is their form factor, and $S(q)$ is the structure factor describing the packing of the primary particles. Assuming nearly spherical primary particles with radius R, we can take

$$V_0 = 4\pi R^3/3 \qquad P(q) = 1/[1 + \sqrt{2}(qR)^2/3]^2$$

$$S(q) = 1 + C(D)/(qR)^D$$

where D is the fractal dimension of the aggregate and $C(D)$ is a constant depending on D:[13] $C(D) = D\Gamma(D - 1)$ sin $[\pi(D - 1)/2]$. Hence, the fit yields three parameters, the background B, the particle radius R, and the fractal dimension D. The fit was usually excellent over 4 orders of magnitude in the intensity and 2 orders of magnitude in q. It also turned out that the constant B was nearly the same for all samples (in the order of 0.02 nm^3). Since this parameter cannot easily be interpreted (and turns out to be a negligible contribution for $q < 3$ nm^{-1}), it will not be discussed further.

Results

The TMOS:$R'Si(OR)_3$ ratio was varied from 9:1 to 6:4. Previous results had shown that a portion of $R'Si(OR)_3$ >40% does not result in stable gel networks, probably because the portion of Q^4 units is then insufficient.[4] Figure 1 shows the gel times for the different mixtures. Gelling becomes drastically slower with an increasing portion of the organically modified precursor. Especially the ISO derivative shows a strong deceleration. (Note that for reasons of availability ISO contains a $Si(OEt)_3$ group instead of $Si(OMe)_3$ in all the other derivatives. It is known that hydrolysis of Si−OEt derivatives is generally slower than that of the corresponding Si−OMe derivatives.) One has to keep in mind that an absolute

(10) Byrne, R. E., Jr. *Anal. Chem.* **1956**, *28*, 126. Johnson, J. B. *Z. Anal. Chem.* **1957**, *154*, 58. Saville, B. *Analyst* **1961**, *86*, 29.

(11) Fratzl, P.; Langmayr, F.; Paris, O. *J. Appl. Crystallogr.* **1993**, *26*, 820.

(12) Fratzl, P.; Vogl, G.; Klaumünzer, K. *J. Appl. Crystallogr.* **1991**, *24*, 588.

(13) Emmerling, A.; Petricevic, R.; Beck, A.; Wang, P.; Scheller, H.; Fricke, J. *J. Non-Cryst. Solids* **1995**, *185*, 240.

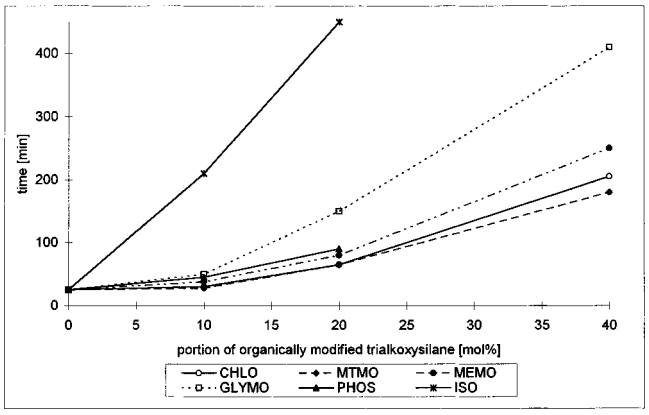

Figure 1. Gel times for the different precursor mixtures.

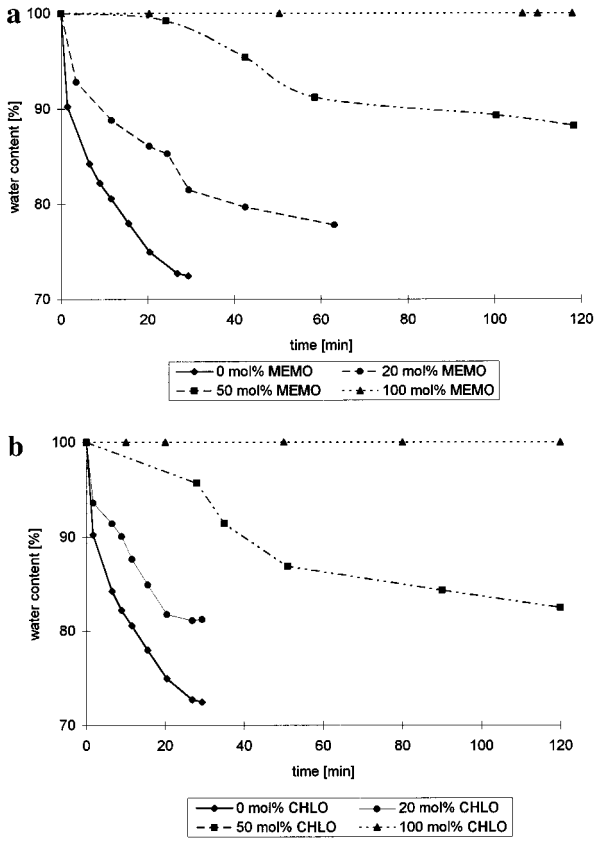

Figure 2. Karl Fischer titration of (a) MEMO and (b) CHLO-containing systems for different portions of R′Si(OR)$_3$ (0−100 mol %). The water content is given in percent of the initial amount.

determination of the gel time is difficult due to its sensitivity to parameters such as stirring velocity, temperature, etc. The gel time also describes only a macroscopic phenomenon. Gelling can be caused by different interactions, such as formation of siloxane bonds, hydrogen bonds, etc. Nevertheless, a qualitative comparison of the gel times of the different mixed-precursor systems and of a pure TMOS system (t_g = 28 min) is possible because the reaction conditions were the same and the systems are chemically similar.

The water consumption during the hydrolysis and condensation reactions up to the gel point was followed by Karl Fischer titrations. Figure 2 shows the change of the water content of MEMO- and CHLO-containing systems up to 120 min after addition of water for

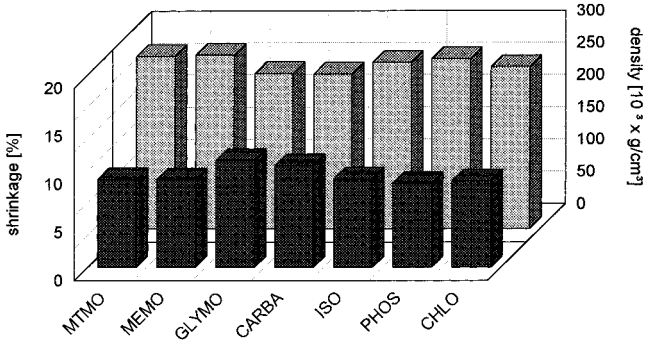

Figure 3. Shrinkage during supercritical drying and bulk density of the organically modified aerogels prepared from 9:1 mixtures of TMOS and R′Si(OR)$_3$.

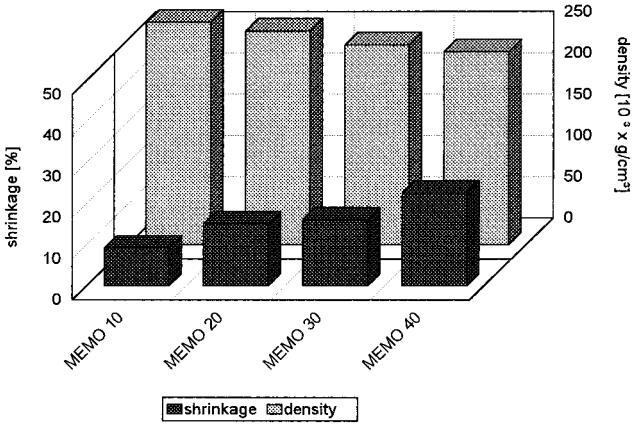

Figure 4. Shrinkage during supercritical drying and bulk density of MEMO-modified aerogels depending on the portion of MEMO in the starting mixture.

mixtures containing different portions of R′Si(OR)$_3$ (0−100 mol %). It is obvious that an increasing portion of R′Si(OR)$_3$ in the starting solution retards the water consumption. For the pure trialkoxysilanes R′Si(OR)$_3$, only negligible hydrolysis was observed during the measuring period. Analogous observations were made for PHOS, GLYMO, and alkyl- or aryl-substituted trialkoxysilanes.

After supercritical drying, all aerogel samples were obtained as cylindrical monoliths. Figure 3 shows the shrinkage during supercritical drying and the bulk density for different organically modified aerogels prepared with a portion of 10 mol % R′Si(OR)$_3$ in the starting silane mixture. Although the theoretical density was adjusted to 0.200 g cm^{-3}, the experimentally determined bulk densities of the final material were between 0.23 and 0.29 g cm^{-3}. The shrinkage was ∼10% for all samples and rather independent of the kind of functional group. Increasing the portion of R′Si(OR)$_3$ in the starting mixture to 40%, as shown for methacrylate-modified samples in Figure 4, led to a large increase of the shrinkage. However, this shrinkage did not result in a higher density as expected, but the density slightly decreased compared with the samples with 10 mol % R′Si(OR)$_3$. This effect can only be explained by the loss of mass during preparation (vide infra).

For comparison, the dependence of shrinkage and experimental bulk density on the portion of R′Si(OR)$_3$ was also investigated for same organofunctional aerogels with lower densities (Figure 5). When the aerogel

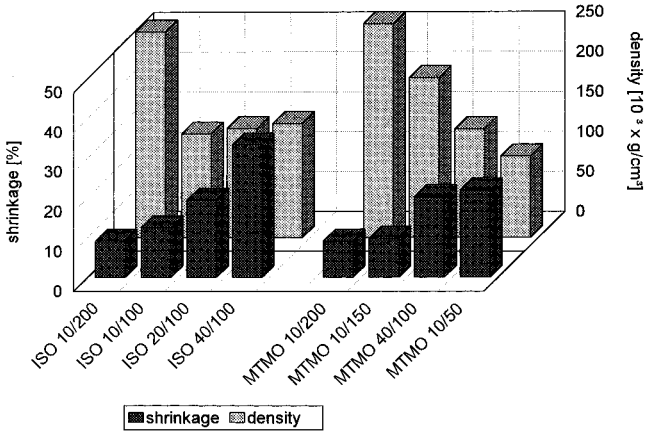

Figure 5. Shrinkage during supercritical drying and bulk density of ISO- and MTMO-modified aerogels depending on the portion of $R'Si(OR)_3$ in the starting mixture and the theoretical density.

Table 3. Characteristic Raman and IR Vibrations

sample	IR literature[14]/ experimental	Raman literature[14]/ experimental	assignment
MTMO	2600/2584	2575/2574	ν(S−H)
MEMO	1725/1713	1725/1699	ν(C═O)
	1639/1639	1640/1641	ν(C═C)
GLYMO	3050/3050	3050/3010	ν(C−O−C) (epoxy)
ISO	2250/1685	—	ν_{as} (NCO)
	1437/1530	—	ν_s (NCO)
CARBA	1730/1690	—	ν(C═O)
	1550/1530	—	ν(N−H)

density is decreased, a larger shrinkage during supercritical drying is expected due to the more filigrane gel network. In the ISO series, the portion of the isocyanato-substituted alkoxysilane in the starting mixture was varied from 10 to 40 mol % at a theoretical density of 0.100 g cm^{-3}. The experimentally found bulk densities were between 0.125 and 0.145 g cm^{-3}, and shrinkage was considerably larger than in the 0.200 g cm^{-3} series. In the MTMO series, the portion of the thio-substituted alkoxysilane in the starting mixture was kept at 10 mol % and the density was varied from 0.200 to 0.100 g cm^{-3}. There was larger shrinkage when the density was lowered, as expected.

The chemical composition of the resulting aerogels was investigated by IR and Raman spectroscopy, elemental analysis, and titration experiments. Characteristic frequencies for the different functionalities are given in Table 3.[14] The spectra showed that in all modified aerogels, the functional groups were retained except the isocyanate groups. The spectroscopic data clearly show that the isocyanate group reacted with methanol to the corresponding carbamate moiety during sol−gel processing or drying. Although in the remainder of this article we will continue to label these aerogels "ISO" according to our nomenclature based on the starting silanes, it should be kept in mind that the final aerogels contain the same functional group as those derived from CARBA. We did not investigate at which stage during the aerogel preparation the isocyanate group was converted into a carbamate group. It is well-known that this reaction occurs readily in the presence of a base catalyst.[15]

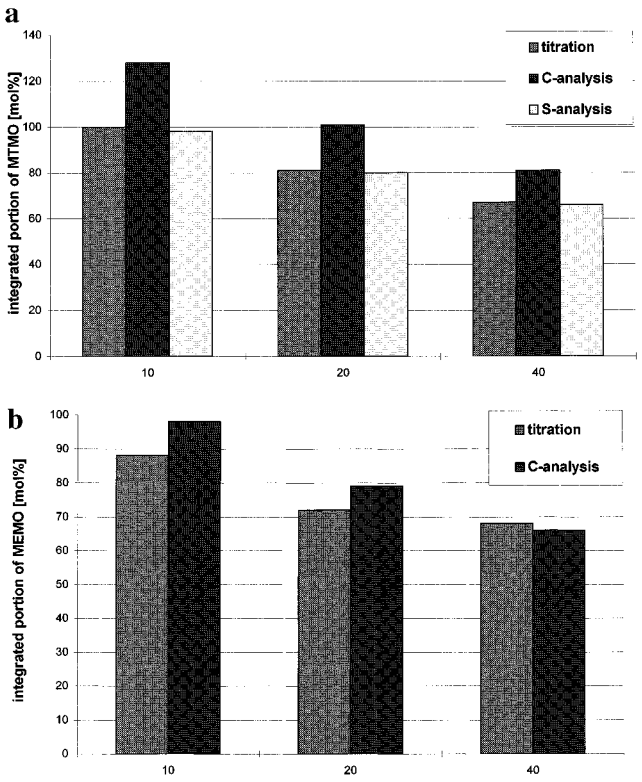

Figure 6. Quantitative analyses of the SH and C═C groups of the MTMO and MEMO samples. The numbers on the abscissa give the portion of $R'Si(OR)_3$ in the starting mixture.

The results of the quantitative analyses of the functional groups by both titration and elemental analysis are presented in Figure 6 for the MEMO and MTMO samples. Similar results were obtained for the other functional groups. The theoretical values of the elemental analyses were calculated assuming 100% integration of the functional organic groups and complete hydrolysis of all alkoxy groups. The fact that the value from the carbon analysis of MEMO 10 is >100% and that the values from the carbon analyses of the MTMO samples are always higher than those from the sulfur analyses shows that hydrolysis was not complete. However, because the portion of residual OMe groups should be in the same range for all samples due to the same reaction conditions, the analyses reflect the qualitative trends that an increasing portion of the $R'Si(OR)_3$ in the starting mixture decreases the incorporated portion of $A(CH_2)_nSi$ groups. For 9:1 mixtures of TMOS and $R'Si(OR)_3$, a complete incorporation was obtained. Only ~60% were incorporated starting from 6:4 mixtures.

The structure of the resulting aerogels was investigated by nitrogen sorption and SAXS measurements. The results are presented in Table 2. The hystereses of the adsorption/desorption isotherms had the same shape as that of unmodified silica aerogels. Therefore, the organically modified samples also have open, cylindrical pores. The specific surface areas of the functionalized samples were significantly lower than for an unmodified silica aerogel, but obviously independent of

(14) Schrader, B. (Ed.) *Raman/Infrared Atlas of Organic Compounds*, 2nd ed.; VCH Weinheim **1988**. Berger, A.; Schenectady, N. Y. U.S. Patent 3,494,951, 1970.

(15) Schwetlick, K.; Noack, R.; Stebner, F. *J. Chem. Soc., Perkin Trans. 2* **1994**, 599.

Table 4. Experimental Density and Pore Volume and Calculated Skeletal Density of the Methacrylate- and Mercapto-Substituted Samples (see text)

sample	exptl. density (d_{bulk}) [g cm^{-3}]	total pore volume [cm^3 g^{-1}]	calcd. skeletal density (d_{skel}) [g cm^{-3}]
unmodified silica aerogel		3.15	2.11
MEMO 10	0.260	2.97	1.14
MEMO 20	0.260	2.86	1.01
MEMO 30	0.249	2.72	0.77
MEMO 40	0.250	2.46	0.65
MTMO 10	0.287	2.65	1.20
MTMO 40	0.262	2.39	0.70
MTMO 10/150	0.200	2.50	0.40
MTMO 40/100	0.136	2.67	0.22

the kind of the organofunctional unit. Except for the CHLO samples, the BET surface areas decrease with an increasing portion of R′Si(OMe)$_3$.

The *C* parameter is an indicator for the polarity of the surface. With the incorporation of 10 mol % of the functionalized precursor, the *C* parameter drops drastically from almost 120 for an unmodified silica aerogel (with a polar surface) to ∼60. For gels with a portion of 40 mol % of the organic units, the *C* parameter levels at ∼40. The decreasing *C* parameter shows that the polarity of the surface decreases with an increasing portion of organic groups in the hybrid aerogels. The kind of organic group only plays an insignificant role. For comparison, a *C* parameter of 30 was observed for unpolar surfaces of modified silicas.[16]

The determination of the porosity or pore radii of aerogel samples by nitrogen sorption is not trivial. As shown by Scherer et al.,[17] the aerogel samples deform during measurement, which results in an underestimation of the specific pore volumina. The magnitude of this effect can be estimated by calculating the skeletal density (d_{skel}) from the experimental bulk density (d_{bulk}) and the total pore volume (V_{pore}) determined by nitrogen sorption ($V_{pore} = 1/d_{bulk} - 1/d_{skel}$). The thus calculated skeletal densities of the methacrylate- and mercapto-substituted samples are given in Table 4. It can clearly be seen that with increasing the portion of MTMO as well as with decreasing the bulk density, the value for the skeletal density drops to more and more unrealistically low values. The same trends were found for the samples with other functional substituents. The skeleton density of unmodified silica aerogels is in the range 2.0−2.2 g cm^{-3}. Although the skeleton density of organically modified silica is expected to be somewhat lower, it can be concluded that the measured pore volumina (and the pore radii calculated from them) of the organically modified aerogels are too small because of increasing compression during the N_2 sorption experiments.

The radius *R* of the primary particles as well as the fractal dimension *D* of their aggregate was determined by SAXS. The scattering curves of selected samples are shown in Figure 7, and the derived parameters are listed in Table 2. Figure 8 shows these SAXS parameters as a function of the BET surface area, determined by nitrogen sorption. Although σ corresponds to the

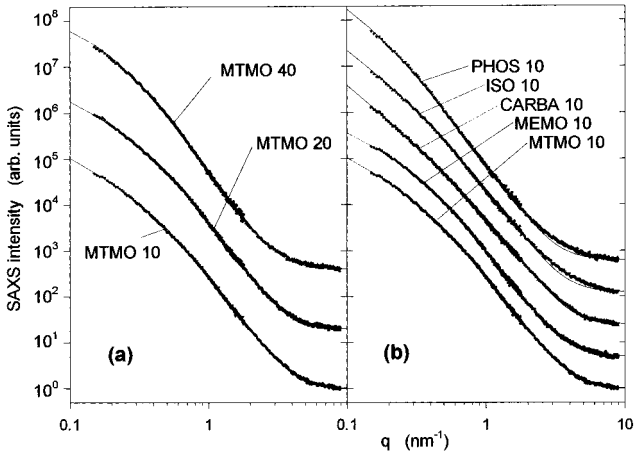

Figure 7. SAXS intensity, $I(q)$, as a function of the scattering vector, q, for selected aerogels. The data are plotted on double-logarithmic scales and are shifted vertically for clarity. The full lines show the fits used to determine particle radius R and fractal dimension D for each sample.

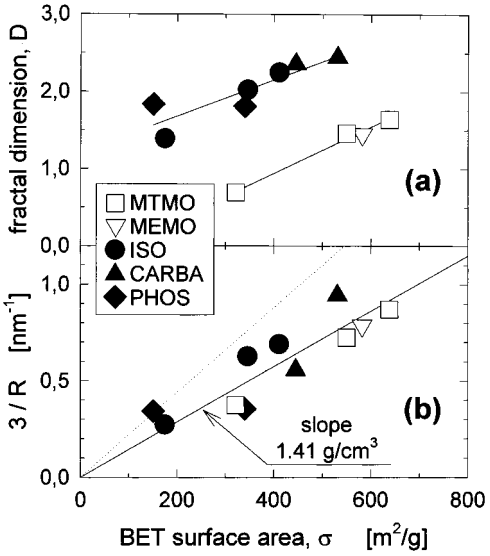

Figure 8. SAXS parameters as a function of the BET surface area per unit mass. Aerogels with different functional groups A are shown by different symbols, as indicated. (a) Fractal dimension of the aerogel network. The full lines are separate linear regressions to the data shown by open and full symbols, respectively. (b) Inverse particle radius, $3/R$. The ratio, $(3/R)/\sigma$, should correspond to the skeletal density of the aerogel. The full line is a linear regression through all data, giving an average skeletal density of ∼1.43 g cm^{-3}. The dotted line corresponds to the skeletal density of pure silica.

internal surface area per unit mass, $3/R$ (that is, the surface-to-volume ratio for a sphere) can be understood as the internal surface area per skeletal unit volume of the aerogel. Figure 8 shows that $3/R$ and are σ roughly proportional, with an average ratio of 1.43 g cm^{-3}. This ratio can be interpreted as the skeletal density, that is, the density of the material within the primary particles. While 1.43 g cm^{-3} is an average value over all samples, the skeletal density varies somewhat between the different aerogels, in particular it appears higher for the ISO- (around 1.7 g cm^{-3}) than for the MTMO- (average 1.2 g cm^{-3}) derived samples. The values of $3/(R\sigma)$ are given in Table 2.

The fractal dimension *D*, which is a measure for the degree of branching of the network formed by the

(16) Lowen, K. W.; Broge, E. C. *J. Phys. Chem.* **1961**, *65*, 16.
(17) Scherer, G. W.; Smith, D. M.; Stein, D. *J. Non-Cryst. Solids* **1995**, *186*, 309.

primary particles,[18] typically increases with increasing σ (see Figure 8a); that is, with a decreasing portion of $A(CH_2)_nSi(OR)_3$ for all aerogel samples. Figure 8a also shows that the aerogels seem to fall into two classes: ISO, CARBA, and PHOS preparations with rather large fractal dimensions, and MTMO and MEMO preparations where the D is much smaller.

Discussion

Although the kind of the functional group A in the silanes used has no severe influence on the network formation process and basic network structure, both of these parameters are distinctly influenced by the portion of $A(CH_2)_nSi(OR)_3$ in the precursor mixture.

The increase of the gel time as well as the slower consumption of water for systems with a higher portion of $R'Si(OR)_3$ shows that under the chosen conditions (base catalysis), $R'Si(OR)_3$ reacts more slowly than the tetraalkoxysilane. We emphasize again that in the present study only trialkoxysilanes $R'Si(OR)_3$ without strongly basic substituents were used. In combination with previous Raman spectroscopic investigations[6] we conclude that the gel network is nearly exclusively built from TMOS, whereas $R'Si(OR)_3$ acts a kind of cosolvent in the beginning of the reaction. Raman spectroscopy also showed that significant consumption of $R'Si(OR)_3$ only takes place after gelation has already occurred.

The structure of aerogels prepared from only $Si(OR)_4$ under basic conditions is described as a network of interconnected chains of weakly branched spherical particles.[19−21] Because $R'Si(OR)_3$ is not involved in the formation of the basic network, there is no principal structural difference when $R'Si(OR)_3/Si(OMe)_4$ mixtures are processed. Only in a later stage of the reaction, when enough acidic surface silanol groups are available, does the $R'Si\equiv$ units condense on the then existing silica network. The existence of spherical primary particles in the aerogels described in this work is, inter alia, supported by the good agreement between the surface areas calculated from the SAXS data with the assumption of spherical particles and the experimental BET surface areas.

Determination of the chemical composition of the final aerogel material allows conclusions to the degree of condensation. For samples with 10 mol % $R'Si(OR)_3$ in the precursor mixture, the incorporation of the organic moieties is almost complete. With an increasing portion of the trialkoxysilane, only 60−70% of the $R'SiO_{3/2}$ groups is incorporated, depending on the kind of $R'Si(OR)_3$ (Figure 6). This result may have three different reasons: First, the gels were aged for 7 days starting from mixing of the precursors, independent of the gel times for the sake of comparability. Longer aging periods for the mixtures with longer gel times may therefore increase the portion of incorporated groups. A second possible reason could be that steric hindrance between the organic groups impedes complete condensation. Third, the two-stage growth model implies that only a certain portion of $R'SiO_{3/2}$ units can be accommodated at the inner surface without changing the basic structure. An excess of $R'Si(OR)_3$ or the corresponding silanols could remain unreacted or undergo self-condensation to small oligomers that are extracted during the supercritical drying process. The assumption of a saturation of the inner surface is supported by the C parameters. When the portion of $A(CH_2)_nSi(OR)_3$ in the starting mixture is increased, the C parameter decreases because the inner surface is successively covered by the organic groups and therefore becomes less polar. A limiting value for the C parameter is reached with 10−20% of $A(CH_2)_nSi(OR)_3$ (Table 3).

The good agreement between the sulfur content determined by titration of the thiol groups and by elemental analysis of the MTMO samples (Figure 6) proves the excellent accessibility of the functional organic groups.

Shrinkage during aging and supercritical drying is qualitatively connected with the stability of the gel network. Shrinkage is large when the aerogel density is low (given the same experimental conditions). Increasing the portion of $R'Si\equiv$ units at a given density also results in a larger shrinkage (Figure 4). This effect gets more pronounced for aerogels with lower density (Figure 5). Shrinkage of the gel body during supercritical drying should result in a proportional increase of the bulk density relative to the theoretical density, because the volume of the aerogel body gets smaller than the volume of the wet gel (i.e., the volume of the precursor solution). In the aerogels prepared in this work, this effect is partially compensated for by the loss of mass, as already discussed in the preceding paragraph.

The main structural changes of the aerogels upon increasing the $A(CH_2)_nSi(OR)_3$ portion in the precursor mixture are the increasing particle sizes and, associated with that, decreasing transparency and specific surface areas, and a larger compression of the network during N_2 adsorption.

The underlying assumption for the following discussion of structural trends is that the structural characteristics of the gel network are preserved when the aged wet gel is supercritically dried by CO_2. Although supercritical drying with alcohols can lead to network rearrangements due to the harsher physical conditions and the cleavage of Si−O−Si bonds by the alcohol, such reactions are less likely with CO_2.[20]

One has to keep in mind that in this work the sol−gel processing of the two-component alkoxysilane mixtures was initiated by adding the whole amount of water and catalyst necessary for the hydrolysis and condensation of both compounds to alcoholic solution of the silanes. The added amount of aqueous 0.01 N NH_4OH solution corresponded to a stoichiometric water/alkoxy group ratio of 1:1. Thus, for a mixture of x parts of $R'Si(OR)_3$ and $(1 - x)$ parts of $Si(OMe)_4$, $(4 - x)$ molar equivalents $[=3x + 4(1 - x)]$ of water were added.

When the reaction is performed in this way, the delayed reaction of the $R'Si(OR)_3$ component has im-

(18) Schmidt, P. W. *J. Appl. Cryst.* **1991**, *24*, 414.
(19) Emmerling, A.; Gross J.; Gerlach, R.; Goswin, R.; Reichenauer, G.; Fricke, J.; Haubold, H.-G. *J. Non-Cryst. Solids* **1990**, *125*, 230. Emmerling, A.; Wang, P.; Popp, G.; Beck, A.; Fricke, J. *J. Phys.* **1993**, *3*, 357.
(20) Wang, P.; Emmerling, A.; Tappert, W.; Spormann, O.; Fricke, J.; Haubold, H.-G. *J. Appl. Crystallogr.* **1991**, *24*, 777.
(21) Schaefer, D. W. *Science* **1989**, *243*, 1023; *MRS Bull.* **1994**, *24(4)*, 49.

mediate consequences on the reaction of $Si(OMe)_4$, because two important reaction parameters are indirectly changed.

(i) Water/Silane Ratio (r_w) and Catalyst Concentration. Because in the first stage of the reaction the second silane $R'Si(OR)_3$ is basically a cosolvent and does not compete for the consumption of water, the tetraalkoxysilane is not faced with a equimolar amount of water and catalyst, but with a relative excess. The relative r_w increases with an increasing portion of $R'Si(OR)_3$ in the starting mixture. For example, in a 9:1 mixture of $Si(OMe)_4$ and $R'Si(OR)_3$, the actual r_w for $Si(OMe)_4$ in the beginning of the reaction is 1.08, in a 8:2 mixture is 1.19, etc. The same arguments apply to the effective catalyst concentration.

(ii) Silane Concentration (C_{TMOS}). To achieve a particular aerogel density, the volume of the reaction solution is adjusted by adding the appropriate amount of alcohol ($d_{aerogel} = [(1 - x)\, m_{SiO_2} + x m_{R'SiO_{3/2}}]/(V_{Si(OMe)_4} + V_{R'Si(OMe)_3} + V_{H_2O} + V_{ROH}$). When the portion of $R'Si(OR)_3$ in the starting mixture is increased, the volume of added alcohol has to be increased to compensate the higher mass of $R'SiO_{3/2}$ relative to SiO_2 and the smaller amount of water (i.e., the concentration of the silanes is decreased and the silane/MeOH ratio gets smaller). Because $R'Si(OR)_3$ is more or less a cosolvent in the beginning of the reaction, the actual concentration of $Si(OMe)_4$ (C_{TMOS}) is even smaller. For example, for the preparation of MTMO10 with a calculated density of 0.200 g cm^{-3}, the TMOS/MeOH ratio in the starting solution is 1:3.06. When the portion of MTMO is increased to 20 or 40% (same calculated density), the ratio decreases to 1:4.41 and 1:8.46.

Therefore, an increasing portion of $R'Si(OR)_3$ in the starting mixture is equivalent to an increased r_w acting on $Si(OMe)_4$, a lower molar concentration of $Si(OMe)_4$ (C_{TMOS}) and a higher catalyst concentration (C_{cat}). The consequences of changing r_w, C_{TMOS}, and C_{cat} in the base-catalyzed reaction of $Si(OR)_4$ are well-known. A higher concentration of ammonia results in larger particles, because it promotes the polycondensation to a higher degree than the hydrolysis rate of the monomer.[22] The rate-limiting step for particle growth is the generation of reactive monomers by TMOS hydrolysis. Therefore, a higher r_w gives larger particles,[23] unless there is no large excess of water. Decreasing the initial concentration of TMOS in methanol (base-catalyzed reaction, $r_w = 2$) was shown to retard the particle growth, although the final particle size was the same.[24]

Thus, the main reason for the larger particles upon increasing the $R'Si(OR)_3/Si(OMe)_4$ ratio in the starting mixture appears to be the increased water/silane ratio (r_w) and the higher catalyst concentration (C_{cat}) acting on TMOS. When a given mass is concentrated in larger particles, the number of particles per volume and thus the surface area become smaller. This situation is what we find experimentally. The pore diameters should become larger, for simple geometric reasons. However, as already discussed, the values for the pore volumina obtained from BET measurements are not reliable because of compression of the network during the N_2 sorption experiments, and therefore this conclusion could not be verified experimentally.

In the previous discussion it was neglected that $R'Si(OR)_3$ also affects the solvent properties, because it is a cosolvent in the network-forming stage. It is well-known that solvents may change the rates of hydrolysis and condensation of alkoxides and thus the structure of the gel network and derived physical properties. The influence of a solvent on these reactions is not readily correlated with its physical properties. Specific solvent effects and the spatial charge distribution in the alkoxides appear to play an important role. The most important parameter is probably the ability of the solvent to reinforce or weaken the hydrogen-bond network.[25] The influence of the functional organic group on the fractal dimension observed in this work (Figure 8) may be caused by such effects. The aerogels prepared from CARBA, PHOS, or ISO have fractal dimensions in the range of those prepared from $Si(OR)_4$ under base-catalyzed conditions[21] (e.g., an aerogel with a bulk density of 0.341 g cm^{-3} prepared from only TMOS under identical conditions and supercritically dried with CO_2 had a fractal dimension of 2.76).[26] Thus, the higher polarity of the functional groups in these silanes, which is reflected in the higher C parameters of the corresponding aerogels, obviously results in only little changes of the solvent properties relative to pure methanol. The dilution of methanol by the less polar MTMO or MEMO seems to interrupt the hydrogen-bond network and thus changes the relative rates of hydrolysis and condensation. In the kinetic growth models, a fractal dimension 2.5 is explained by the predominance of monomer−cluster condensation over cluster−cluster condensation.[21] This predominance happens if hydrolysis is slow compared with condensation. The hydrolysis/condensation ratio is obviously increased by the addition of MEMO or MTMO. Because the gel times of these systems are rather similar to the others, the addition of these silanes appears to accelerate the hydrolysis reaction relative to condensation. Cluster−cluster aggregation is thus rendered more favorable.

Conclusions

We have shown in this paper that a variety of organofunctional groups can be incorporated into silica aerogels starting from $A(CH_2)_nSi(OR)_3/Si(OR)_4$ mixtures. In the investigated series of organofunctional alkoxides (Scheme 1), only the isocyanato group did not survive the preparation conditions and was converted to a carbamato group by reaction with methanol. The organic groups are completely incorporated if the portion of $A(CH_2)_nSi(OR)_3$ in the starting mixture does not exceed 10%. All spectroscopic and chemical evidence is consistent with the notion that the organic groups are located at the inner surface of the aerogel and are accessible. This insight opens new opportunities for the use of organically modified silica aerogels as sensors, catalysts, etc.

(22) Matsoukas, T.; Gulari, E. *J. Colloid Interface Sci.* **1988**, *124*, 252.
(23) Keefer, K. T. *Mater. Res. Soc. Symp. Proc.* **1986**, *73*, 295.
(24) Himmel, B.; Bürger, H.; Gerber, T.; Olbertz, A. *J. Non-Cryst. Solids* **1995**, *185*, 56.
(25) Zerda, T. W.; Hoang, G. *Chem. Mater.* **1990**, *2*, 372.
(26) Schwertfeger, F. *Diplomarbeit*, Universität Würzburg, 1991.

Beyond that, the structural investigation of the aerogels also allowed new insight into the network formation and network structure in two-component sol−gel systems. In a series of organically modified silica aerogels of equal density prepared by base-catalyzed sol−gel processing of $R'Si(OR)_3/Si(OMe)_4$ mixtures, an increasing portion of $R'Si(OR)_3$ has the same kinetic effects on the hydrolysis and condensation reactions and the same structural consequences for the network formation as decreasing the bulk density of an aerogel obtained from the one-component TMOS system. All structural features can be explained if one assumes that in the network-forming stage of the hydrolysis and condensation reaction the organotrialkoxysilane acts as a cosolvent.

Acknowledgment. This work was funded by the Fonds zur Förderung der wissenschaftlichen Forschung (FWF), Vienna, and the Hoechst AG, Frankfurt. We thank Profs. Jochen Fricke (Physics Institute, University of Würzburg) and Wolfgang Kiefer (Institute of Physical Chemistry, University of Würzburg) and their co-workers for fruitful cooperations and discussions.

CM980706G